

Sites for Methane Activation on Lithium-Doped Magnesium Oxide Surfaces**

Karolina Kwapien, Joachim Paier, Joachim Sauer,* Michael Geske, Ulyana Zavyalova, Raimund Horn,* Pierre Schwach, Annette Trunschke,* and Robert Schlögl

Dedicated to the MPI für Kohlenforschung on the occasion of its centenary

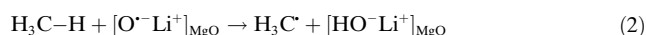
Abstract: Density functional calculations yield energy barriers for H abstraction by oxygen radical sites in Li-doped MgO that are much smaller ($12 \pm 6 \text{ kJ mol}^{-1}$) than the barriers inferred from different experimental studies ($80\text{--}160 \text{ kJ mol}^{-1}$). This raises further doubts that the Li^+O^- site is the active site as postulated by Lunsford. From temperature-programmed oxidative coupling reactions of methane (OCM), we conclude that the same sites are responsible for the activation of CH_4 on both Li-doped MgO and pure MgO catalysts. For a MgO catalyst prepared by sol–gel synthesis, the activity proved to be very different in the initial phase of the OCM reaction and in the steady state. This was accompanied by substantial morphological changes and restructuring of the terminations as transmission electron microscopy revealed. Further calculations on cluster models showed that CH_4 binds heterolytically on $\text{Mg}^{2+}\text{O}^{2-}$ sites at steps and corners, and that the homolytic release of methyl radicals into the gas phase will happen only in the presence of O_2 .

Taylor's active site concept^[1] has stimulated catalysis research over almost a century, but it took many decades until surface science identified low-coordinated atoms at step edges as active sites of metal catalysts.^[2] Subsequently, the complex nature of active sites at supported metal^[3] or metal oxide catalysts^[4,5] has been revealed by combined experimental and computational studies. With the raw material shift

in chemical industry to natural gas, there is renewed interest in the formation of higher hydrocarbons, for example by oxidative coupling of methane (OCM):^[6]



The simplest catalysts for this reaction, among a large number of complex solid oxides, is Li-doped MgO.^[7] Early, Lunsford proposed that the active sites are O^- radicals neighbored to Li^+ , with Li^+O^- formally replacing $\text{Mg}^{2+}\text{O}^{2-}$,^[8] and that the C–H bond is activated by homolytic splitting involving hydrogen atom transfer to the O^- sites:^[9]



However, there is also evidence that the Li^+O^- site may not be the active site and that the C–H bond may be heterolytically split,^[6] as Lunsford already mentioned in his 1995 review.^[7] Recently, crucial ENDOR experiments showed that in none of the powder catalysts that were run under an OCM atmosphere Li^+O^- centers could be found,^[10,11] although they were detectable in Li-doped MgO single crystals prepared by arc fusion of $\text{MgO}/\text{Li}_2\text{CO}_3$.^[10] Instead, by careful multi-method characterization,^[11,12] Li addition was found to lead to restructuring of the MgO surface exposing steps and corner sites and high-index crystallographic surfaces alien to pristine MgO. Studies of thin MgO films by surface science techniques reached the same conclusion.^[10]

Herein, we provide theoretical and further experimental evidence that the Li^+O^- site is not the active site and conclude that the activity of OCM catalysts is connected with morphological features of the crystallites that form under reaction conditions and depend on the synthesis process. Lunsford already points to a discrepancy^[7] between the measured apparent activation energy for the formation of methyl radicals ($96 \pm 8 \text{ kJ mol}^{-1}$)^[13] and quantum chemical calculations. In 2005 Catlow et al. used density functional theory and periodic models to calculate the energy barrier of H abstraction by an O^- site at the (001) surface of Li-doped MgO.^[14] The barrier obtained, 74 kJ mol^{-1} , is more or less in apparent agreement with the above value and reported barriers of 85 kJ mol^{-1} (CH_4/CD_4 isotope exchange)^[15] and 90 kJ mol^{-1} (C_2 hydrocarbon formation).^[16] Microkinetic simulations yielded significantly higher values, namely 147 kJ mol^{-1} .^[17] More recently, Li-doped MgO catalysts have been found unstable under reaction conditions, and after 24 h

[*] Dr. K. Kwapien, Dr. J. Paier, Prof. Dr. J. Sauer
Institut für Chemie, Humboldt-Universität
Unter den Linden 6, 10099 Berlin (Germany)
E-mail: sek.qc@chemie.hu-berlin.de

Dr. M. Geske, Dr. U. Zavyalova, Prof. Dr. R. Horn, P. Schwach,
Dr. A. Trunschke, Prof. Dr. R. Schlögl
Fritz-Haber-Institut der Max-Planck-Gesellschaft
Faradayweg 4-6, 14195 Berlin (Germany)

Prof. Dr. R. Horn
Current address: Institut für Chemische Reaktionstechnik
Technische Universität Hamburg-Harburg
Eißendorfer Strasse 38, 21073 Hamburg (Germany)

[**] This work has been supported by Deutsche Forschungsgemeinschaft within the Cluster of Excellence "Unifying Concepts in Catalysis". We thank Wiebke Frandsen for recording of MgO images by transmission electron microscopy. K.K. thanks the International Max Planck Research School "Complex Surfaces in Materials Science" for a fellowship. J.S. is grateful for a Miller Visiting Professorship at Berkeley, during which parts of this paper have been written.

Supporting information for this article is available on the WWW under <http://dx.doi.org/10.1002/anie.201310632>.

time on stream barriers between 89 and 160 kJ mol⁻¹ have been measured, depending on the synthesis method.^[18]

We report quantum chemical calculations that go beyond limitations of previous work as far as models for the active site, localization method of the transition structure and accuracy of the quantum chemical approach are concerned. Our predicted energy barriers, between 7 ± 6 and 27 ± 6 kJ mol⁻¹, are surprisingly low compared to the experimental results, which suggests that the Li⁺O⁻ site is not the active site.

Support for this conclusion comes from temperature programmed reaction experiments, which show that on both Li-doped MgO and pure MgO catalysts conversion of CH₄ and O₂ starts at about 410 °C and formation of C₂ species at about 540 °C. The difference is that in this initial phase of the reaction Li-MgO is far more active and selective in forming C₂ coupling products than pure MgO. We conclude that the reaction pathways are the same for both materials and that the same active sites are present. The role of Li-doping is increasing the number of active sites, which is most likely due to changes of the morphology connected with the formation of a larger number of low-coordinate O²⁻ ions at edges, corners, and kinks.^[10–12]

For further kinetic studies, a pure MgO model catalyst has been synthesized by a sol–gel process and characterized by transmission electron microscopy (TEM). The catalyst activity was very different in the initial phase of the OCM reaction and in the steady state, and this was accompanied by substantial morphological changes. In the steady state, the apparent activation barrier for CH₄ conversion is 133 ± 2 kJ mol⁻¹, within the 80 to 160 kJ mol⁻¹ range inferred before for Li-doped MgO.^[15–18]

To further explore possible sites for CH₄ activation on Li-free MgO catalysts, we have examined the interaction of CH₄ with morphological defects (steps, corners) by DFT. The calculations showed that the C–H bond adds heterolytically onto an Mg²⁺O²⁻ ion pair, but that homolytic release of methyl radicals in the gas phase is only likely in the presence of O₂.

Figure 1 shows both cluster and periodic models adopted for the Li⁺O⁻ site at the MgO (001) surface terrace. The LiO(MgO)₈ cluster has the topology of a two-layer cut-out from the surface. In the constraint cluster model we limit structure relaxation to the Li⁺ and O⁻ ions in the center of the cluster, whereas the positions of all other atoms are fixed at the positions they have in the MgO bulk. In our four-layer slab model, all of the ion positions are relaxed except those in the two bottom layers. The B3LYP hybrid density functional^[19,20] has been used, which reproduces within 6 kJ mol⁻¹ CCSD(T) coupled cluster results of C–H bond splitting barriers for CH₄ at O⁻ sites of (MgO)_n⁺ clusters.^[21,22] CCSD(T) is considered to be chemically accurate. For gas-phase metal oxide clusters featuring radical sites, B3LYP has also been shown to correctly predict for which clusters hydrogen abstraction can be observed by mass spectrometry and for which not.^[21,23]

Figure 1 shows the geometric structures of the active site and the transition state (for bond distances, see the Supporting Information) as well as the spin densities. In the transition

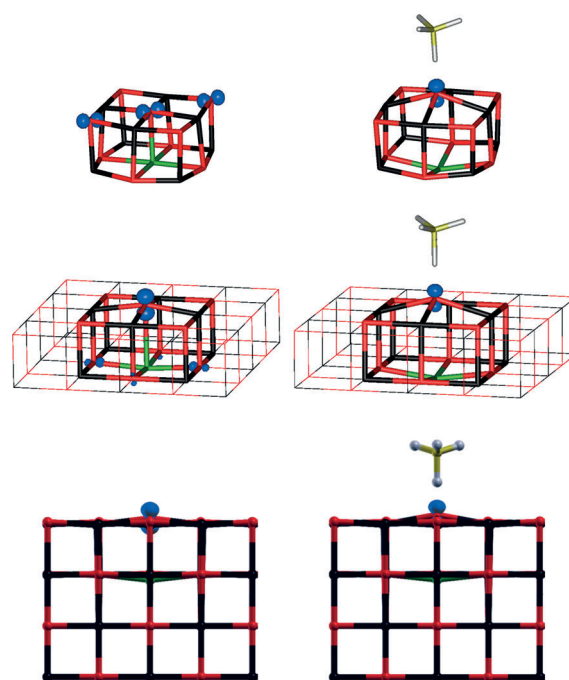


Figure 1. From top to bottom: Cluster model, constraint cluster model embedded in a periodic array of point charges, and periodic model of an Li⁺O⁻ site on the MgO(001) terrace. Left: active site structure, right: transition structure for H abstraction from CH₄. O red, Mg black, Li green, C yellow, H gray, spin density blue.

structure, the spin localizes at the surface oxygen ion above the lithium ion for all models. In the initial state, the unconstrained model shows delocalization over two additional oxygen ions. This is rectified when embedding the cluster in a periodic array of point charges and a finite number of full ion pseudopotentials, which also lowers the apparent barrier by 20 kJ mol⁻¹ (Table 1, terrace). The periodic model barrier is only 14 kJ mol⁻¹ lower than the embedded cluster barrier and 12 kJ mol⁻¹ of this difference are due to relaxing a larger number of atoms in the periodic model. This we gather from the single point embedded cluster result at the structure obtained for the periodic model.

We conclude that for Li⁺O⁻ terrace sites, the activation barrier is as low as 12 ± 6 kJ mol⁻¹ (Table 1). The much higher

Table 1: Apparent energy barriers (kJ mol⁻¹, B3LYP functional) for hydrogen abstraction from methane at Li⁺O⁻ sites at the MgO(001) terrace and corner sites.

Model	Terrace	Corner 1	Corner 2
cluster, free	61.3	18.9	21.7
cluster, constraint ^[a]	57.3	22.8	22.4
cluster, embedded ^[a,b]	41.2 [29.3] ^[c]	29.8	29.5
periodic model	26.8 (35.1) ^[d]	(23.7) ^[d]	(52.2) ^[d]
+ dispersion	12.3 (26.8) ^[d]	(21.8) ^[d]	(42.1) ^[d]

[a] Only the surface O ion and the Li ion beneath are allowed to move.

[b] Periodic electrostatic embedded cluster model.^[24] [c] Single-point calculation at the B3LYP structure obtained for the periodic model.

[d] Single-point hybrid B3LYP(cluster):PBE(periodic) calculations at the PBE structure obtained for the periodic model.

previous estimates (74 kJ mol^{-1})^[14] we ascribe to neglect of dispersion and an incomplete optimization for the transition structure in that study. For different morphological positions, for example, at corners, depending on the model the barriers may be 5 kJ mol^{-1} lower ("corner 1") or 15 kJ mol^{-1} higher ("corner 2") than for terrace sites (Table 1, last row, values in brackets).

Temperature-programmed reaction measurements were carried out on 150 mg of pure MgO and 5 wt% Li-doped MgO, both prepared by gel combustion synthesis as described previously.^[11] Briefly, glycerol as fuel was mixed with aqueous solutions of LiNO_3 and $\text{Mg}(\text{NO}_3)_2$. After water was removed by evaporation, a highly energetic combustible gel was obtained in which Li^+ and Mg^{2+} ions were molecularly dispersed. Upon ignition, the gel combusted vigorously to the oxides followed by rapid thermal quenching. However, despite rapid combustion and rapid thermal quenching, which may lead to structures far from equilibrium, it was not possible to detect Li^+O^- defects in any material obtained this way. As discussed in detail in Ref. [11], CW-EPR, ENDOR and DR-UV/Vis, all established diagnostic methods for Li^+O^- defects,^[10,25] were applied, but no method could detect Li^+O^- defects in any of our materials. Using optical spectroscopy morphological defects, that is, low-coordinate O^{2-} ions at edges, corners, and kinks of the MgO surface have been identified that arise from the volatilization of the Li component being initially present in the MgO sample as solid solution.

The pure MgO and the Li-doped MgO catalysts were subjected to a temperature ramp of 3 K min^{-1} in a plug flow reactor using an OCM mixture consisting of $10 \text{ mL min}^{-1} \text{ CH}_4$, $1.25 \text{ mL min}^{-1} \text{ O}_2$, and $2 \text{ mL min}^{-1} \text{ Ar}$ as internal standard. Figure 2 shows the results for CH_4 , O_2 , C_2H_4 , and C_2H_6 ; the corresponding data for CO and CO_2 formation are given in the Supporting Information. On both catalysts, O_2 and CH_4 conversion into CO_2 commences at about 410°C with CO_2 as the far dominant oxidation product. Arrhenius plots on O_2 consumption (see the Supporting Information) give very similar apparent activation energies of 205 and 184 kJ mol^{-1} on pure MgO and Li-MgO, respectively, indicating a similar mechanism of initial O_2 activation on both materials. CO, C_2H_6 , and C_2H_4 formation begins on both materials at 540°C , but Li-MgO is far more active and selective in forming C_2 coupling products than pure MgO.

TEM investigations of MgO particles obtained by a sol-gel process show substantial morphology changes during time on-stream. Figure 3 shows a TEM image of the MgO catalyst used for the data in Table 2 after 6 h and after 230 h time on-stream. Careful transfer into the TEM under exclusion of air reveals the restructuring of the termination, losing the (100)

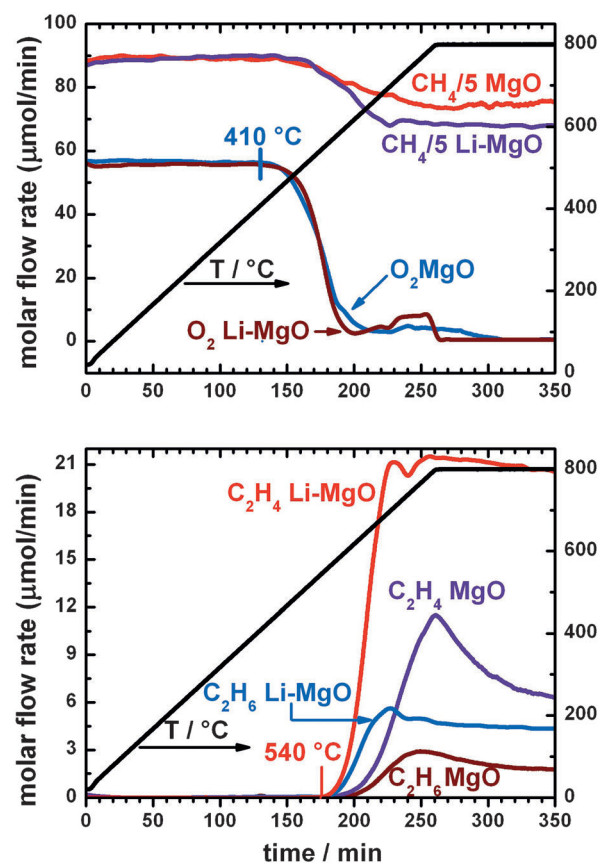


Figure 2. Flow rates of CH_4 , O_2 (top), and C_2H_6 , C_2H_4 (bottom) in temperature-programmed oxidative methane coupling on pure MgO and 5 wt% Li-doped MgO.

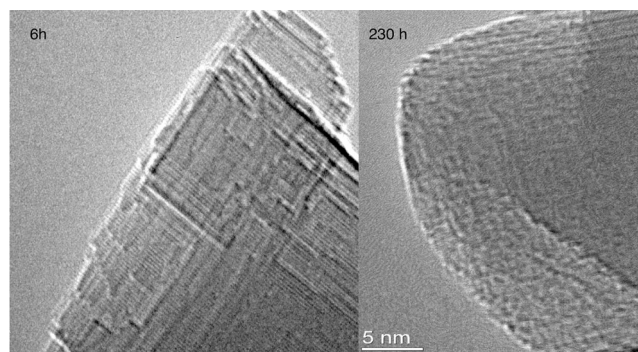


Figure 3. TEM images of pure MgO after 6 h (left) and after reaching steady state (230 h, right).

orientation from the fresh MgO for a rough termination structure. In both cases, substantial numbers of non-terrace sites are present that expose Mg sites with lower coordination than fivefold and may serve as active sites. The diffuse termination of the 230 h used sample indicates the presence of additional terminating species, such as OH groups that may block many of such sites for methane adsorption.

Concomitantly with the morphological changes, the catalyst activity was very different in the initial phase of the OCM reaction and the steady state (Table 2). CH_4 conversion

Table 2: Performance of the Li-free MgO catalyst in the oxidative coupling of methane.

	Rate [$\mu\text{mol s}^{-1} \text{ g}_{\text{cat}}^{-1}$]	Rate [$\mu\text{mol s}^{-1} \text{ m}_{\text{cat}}^{-2}$]	X(CH_4) [%] ^[a]	S(C_2) [%] ^[a]
initial state	214.4	5.56	26.04	29.84
final state	8.57	1.26	4.70	13.85

[a] X: conversion, S(C_2): selectivity to ethane and ethylene.

and C₂ selectivity changed from 26 and 30 %, respectively, to 5 and 14 %, respectively. This is connected with substantial restructuring as the rate per catalyst weight reduces by factor of 25, whereas the rate per surface area reduces by a factor of 4.4 only.

As a model for morphological defects (steps, corners) on Li-free MgO catalysts we adopt the (MgO)₉ cluster. Figure 4

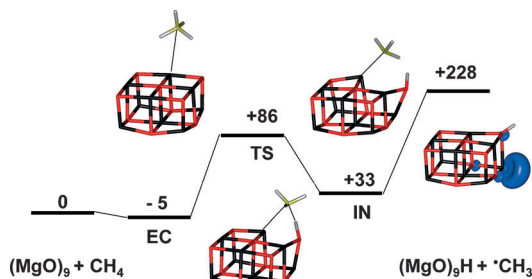
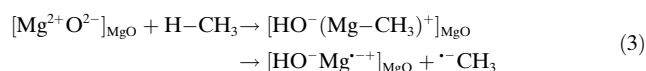


Figure 4. Reaction energy diagram for chemisorption of CH₄ onto corner/edge sites of a Mg₉O₉ cluster showing C–H bond addition on an Mg²⁺O²⁻ pair. B3LYP energies are given in kJ mol⁻¹, for energies including zero-point vibrational contributions see Supporting Information. EC encounter complex, TS transition state, IN intermediate; colors as in Figure 1.

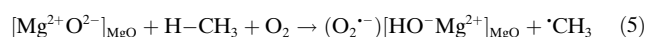
shows the energy diagram for the reaction with CH₄. Chemisorption occurs by heterolytic addition of the C–H bond onto an Mg²⁺O²⁻ pair:



The surface species formed are an OH group (by protonation of O²⁻) and a Grignard type Mg-methylate (by addition of CH₃⁻ to Mg²⁺). Such reactions have been discussed before,^[26] for example, for low-coordinate sites on γ-alumina.^[27] The barrier for this slightly endothermic reaction is at the low side of typical barriers for OCM reactions, but releasing a methyl radical to the gas phase is barrierless but needs as much as 228 kJ mol⁻¹. However, the unpaired electron formed in this reaction facilitates O₂ chemisorption as a superoxide species:



This reaction is very exothermic (−191 kJ mol⁻¹,^[28] so that the overall process:



becomes almost thermal neutral (ΔE = 37 kJ mol⁻¹). There is, of course, an entropy penalty, as two gas-phase species are converted into one, but reaction (5) also yields a superoxo surface species that is more reactive than O₂ in the gas phase.

Future studies should also consider possible reactions of dioxygen with the Mg-methylate, which may also lead to methyl radicals and surface peroxo species.^[29,30] Pros and cons of reaction (5) as a possible source of methyl radicals in the

OCM process have already been discussed.^[7] Our model calculations are indeed strong evidence that heterolytic chemisorption of CH₄ on MgO in the presence of O₂ becomes energetically feasible on morphological defects such as steps or corners and plays a significant role in the OCM process. Currently, we are further investigating possible mechanisms based on this idea. Whereas quantum chemical calculations on realistic models as presented here can provide reliable information on individual reaction steps, comparison with experimental kinetic data requires micro-kinetic simulations that use these data as input.

Our experiments (see also Ref. [31]) in combination with theoretical studies suggest a different role of non-reducible oxides as catalysts on methane activation. Their role is not to provide and receive back electrons as with reducible oxide catalysts, but merely to stay inert with its own electronic system and just bring together the reactants allowing exchanging redox equivalents directly between themselves. Such a function is expressed in the designation “catalyst” meaning the bringing together of reactants.

Received: December 7, 2013

Revised: February 19, 2014

Published online: April 23, 2014

Keywords: active sites · C–H activation · density functional calculations · Li-doped MgO · magnesium oxide

- [1] H. S. Taylor, *Proc. R. Soc. London Ser. A* **1925**, 108, 105–111.
- [2] T. Zambelli, J. Wintterlin, J. Trost, G. Ertl, *Science* **1996**, 273, 1688–1690.
- [3] M. Behrens, F. Studt, I. Kasatkin, S. Kühl, M. Hävecker, F. Abild-Pedersen, S. Zander, F. Girgsdies, P. Kurr, B.-L. Kniep, M. Tovar, R. W. Fischer, J. K. Nørskov, R. Schlögl, *Science* **2012**, 336, 893–897.
- [4] M. V. Ganduglia-Pirovano, C. Popa, J. Sauer, H. L. Abbott, A. Uhl, M. Baron, D. Stacchiola, O. Bondarchuk, S. Shaikhutdinov, H.-J. Freund, *J. Am. Chem. Soc.* **2010**, 132, 2345–2349.
- [5] K. Amakawa, L. Sun, C. Guo, M. Hävecker, P. Kube, I. E. Wachs, S. Lwin, A. I. Frenkel, A. Patlolla, K. Hermann, R. Schlögl, A. Trunschke, *Angew. Chem.* **2013**, 125, 13796–13800; *Angew. Chem. Int. Ed.* **2013**, 52, 13553–13557.
- [6] E. V. Kondratenko, M. Baerns, *Handbook of Heterogeneous Catalysis, Vol. 6* (Ed.: H. K. G. Ertl, F. Schüth, J. Weitkamp), Wiley-VCH, Weinheim, **2008**.
- [7] J. H. Lunsford, *Angew. Chem.* **1995**, 107, 1059–1070; *Angew. Chem. Int. Ed. Engl.* **1995**, 34, 970–980.
- [8] D. J. Driscoll, W. Martir, J. X. Wang, J. H. Lunsford, *J. Am. Chem. Soc.* **1985**, 107, 58–63.
- [9] T. Ito, J. Wang, C. H. Lin, J. H. Lunsford, *J. Am. Chem. Soc.* **1985**, 107, 5062–5068.
- [10] P. Myrach, N. Nilius, S. V. Levchenko, A. Gonchar, T. Risse, K. P. Dinse, L. A. Boatner, W. Frandsen, R. Horn, H. J. Freund, R. Schlögl, M. Scheffler, *ChemCatChem* **2010**, 2, 854–862.
- [11] U. Zavyalova, G. Weinberg, W. Frandsen, F. Girgsdies, T. Risse, K. P. Dinse, R. Schlögl, R. Horn, *ChemCatChem* **2011**, 3, 1779–1788.
- [12] U. Zavyalova, M. Geske, R. Horn, G. Weinberg, W. Frandsen, M. Schuster, R. Schlögl, *ChemCatChem* **2011**, 3, 949–959.
- [13] M. Xu, C. Shi, X. Yang, M. P. Rosynek, J. H. Lunsford, *J. Phys. Chem.* **1992**, 96, 6395–6398.

- [14] C. R. A. Catlow, S. A. French, A. A. Sokol, J. M. Thomas, *Philos. Trans. R. Soc. London Ser. A* **2005**, 363, 913–936.
- [15] V. S. Muzykantov, A. A. Shestov, H. Ehwald, *Catal. Today* **1995**, 24, 243–244.
- [16] M. Y. Sinev, V. Y. Bychkov, V. N. Korchak, O. V. Krylov, *Catal. Today* **1990**, 6, 543–549.
- [17] J. Sun, J. W. Thybaut, G. B. Marin, *Catal. Today* **2008**, 137, 90–102.
- [18] S. Arndt, U. Simon, S. Heitz, A. Berthold, B. Beck, O. Görke, J. D. Epping, T. Otremba, Y. Aksu, E. Irran, G. Laugel, M. Driess, H. Schubert, R. Schomäcker, *Top. Catal.* **2011**, 54, 1266–1285.
- [19] A. D. Becke, *J. Chem. Phys.* **1993**, 98, 5648–5652.
- [20] C. Lee, W. Yang, R. G. Parr, *Phys. Rev. B* **1988**, 37, 785–789.
- [21] K. Kwapien, M. Sierka, J. Döbler, J. Sauer, *ChemCatChem* **2010**, 2, 819–826.
- [22] K. Kwapien, Active Sites for Methane Activation in MgO and Li-doped MgO, Doctoral thesis, Humboldt University, **2011**.
- [23] S. Feyel, J. Döbler, R. Höckendorf, M. K. Beyer, J. Sauer, H. Schwarz, *Angew. Chem.* **2008**, 120, 1972–1976; *Angew. Chem. Int. Ed.* **2008**, 47, 1946–1950.
- [24] A. M. Burow, M. Sierka, J. Döbler, J. Sauer, *J. Chem. Phys.* **2009**, 130, 174710.
- [25] M. M. Abraham, Y. Chen, L. A. Boatner, R. W. Reynolds, *Phys. Rev. Lett.* **1976**, 37, 849–852.
- [26] C. Copéret, *Chem. Rev.* **2010**, 110, 656–680.
- [27] R. Wischert, P. Laurent, C. Copéret, F. Delbecq, P. Sautet, *J. Am. Chem. Soc.* **2012**, 134, 14430–14449.
- [28] D. Ricci, G. Pacchioni, P. V. Sushko, A. L. Shluger, *Surf. Sci.* **2003**, 542, 293–306.
- [29] A. G. Davies, B. P. Roberts, *Acc. Chem. Res.* **1972**, 5, 387–392.
- [30] P. J. Bailey, R. A. Coxall, C. M. Dick, S. Fabre, L. C. Henderson, C. Herber, S. T. Liddle, D. Loroño-González, A. Parkin, S. Parsons, *Chem. Eur. J.* **2003**, 9, 4820–4828.
- [31] P. Schwach, W. Frandsen, M. Willinger, R. Schlögl, A. Trunschke, in preparation **2013**.